scientific reports

Check for updates

OPEN

Complex network analysis of mobility dynamics in Seoul during the COVID-19 pandemic 2020–2022

Zeyu Hu[1], Manjun Yu[1], Youngook Jang[2], Sourya Shrestha[3], Jaehun Jung[4]✉ & Youngji Jo[5]✉

Recent advances in geolocated data enable quantitative analysis of human mobility, critical for urban planning and epidemic control. This study examines mobility dynamics in Seoul during the COVID-19 pandemic, where minimal lockdown measures allowed relatively natural movement patterns, offering insights for managing viral spread with reduced socioeconomic disruption. We analyzed the Seoul "Living Mobility" dataset (January 2020–December 2022), which contains monthly origin-to-destination flows among 424 sub-districts ("dong") in 25 districts ("gu"). We constructed a directed and weighted mobility network based on monthly trips between every pair of dongs. We assessed (i) local node intensity via weighted density within and across districts, (ii) global connectivity through distribution of node strengths, (iii) node clusters via community detection with the Infomap community-detection algorithm, and (iv) the top and bottom 10 hub nodes using weighted PageRank centrality. From 2020 to 2022, within-gu weighted density increased by 21.7%, and across-gu density by 13.0%. Node strength distribution showed 138 high-mobility dongs (33%) driving 56% of total flows. Community detection identified 11 clusters transcending district boundaries, with within-community mobility 2–5 times higher than cross-community flows. High-mobility hubs, such as Yeoksam-dong (Gangnam-gu) and Yeoui-dong (Yeongdeungpo-gu), exhibited up to 70 times more movement than peripheral areas. Seoul's mobility network remained fully connected yet highly heterogeneous during the COVID-19 pandemic years, with central hubs and clusters dominating movement. The rising saturation of within-dong flows reflects intensified local interactions, highlighting the growing importance of clustering and localized hotspots in driving future transmission risks. Targeting interventions at the 138 high-mobility dongs—and at bridges between their communities—can optimize disease control while minimizing disruption. Low-mobility dongs highlight potential service access disparities, guiding tailored interventions for equitable urban planning and public health strategies.

Recent advances in geolocated data collection have opened unprecedented possibilities for quantitatively examining both individual and collective human mobility patterns[1–3]. These patterns bear directly on numerous applications, including urban planning and epidemic modeling[2–7]. The COVID-19 pandemic has underscored the critical relationship between human movement and disease transmission, particularly in densely populated urban environments[8]. Public health officials typically use conventional disease surveillance to identify transmission hotspots, but case reporting data are often aggregated by administrative unit and reflect testing locations rather than actual transmission sites[9]. In this regard, analyzing mobility networks can address the gap by elucidating contact patterns and interaction intensity among urban populations[10].

Prior research has examined how COVID-19 reshaped mobility in various cities, including structural network changes[11], population flow analysis[12,13], and the adaptation of individual travel behaviors[14]. These studies showed that COVID-19 weakened urban-core centrality and overall network density, prompting a shift toward more localized community structures. Most analyses focused on 2020, with only a few extending to 2019–2023. Mobility networks generally experienced a V-shaped trajectory—an abrupt collapse (e.g., Germany's 40% plunge in March 2020[11]) followed by a partial, uneven rebound that often stopped short of pre-pandemic vitality (Shenzhen's urban-vitality index remained 14% below 2019 in mid-2023[15]). Even where high-flow hubs recovered quickly, pandemic-era fragmentation persisted—U.S. neighborhood isolation stayed elevated through

[1]Department of Statistics, University of Connecticut, Storrs, Connecticut, USA. [2]Korea Institute for International Economic Policy, Sejong, South Korea. [3]Department of Epidemiology, Johns Hopkins Bloomberg School of Public Health, Baltimore, Maryland, USA. [4]Department of Preventive Medicine, Korea University College of Medicine, Seoul, South Korea. [5]Department of Public Health Sciences, School of Medicine, University of Connecticut, Farmington, Connecticut, USA. ✉email: eastside1st@gmail.com; jo@uchc.edu

2022—indicating that such shocks do not simply scale mobility down uniformly[16]; they rewire urban systems in ways that privilege local, infrastructure-dependent movement and leave a sustained impact on cross-city connectivity.

Unlike many global cities that enforced strict lockdowns, South Korea pursued testing, contact tracing, and targeted interventions rather than imposing sweeping mobility restrictions[17]. This approach enables the observation of urban movement patterns that remain relatively undistorted by policy mandates. In Seoul and Gyeonggi Province specifically, Kim and Jun (2022) investigated how the pandemic affected the broader directionality of mobility networks - centripetal (pulling to the center) vs. centrifugal (pushing outward) mobility forces - in the metropolitan area from February to August 2020[18]. While mobility data has been extensively collected, no study has systematically identified specific network properties at local administrative divisions (dongs)—such as community clusters and hub locations—in an extended period that offers insights to help design localized and equitable pandemic responses.

This research aims to identify key hubs and community clusters within Seoul's (home to over 9.5 million residents) COVID-19-era mobility network to inform targeted public health measures and urban planning strategies. Because Seoul's pandemic response relied on more moderate and targeted interventions (such as a "3T" strategy – Test, Trace, and Treat) than imposing complete lockdowns, our results provide an informative benchmark for policymakers and public health officials seeking strategies that curb viral spread while minimizing disruptions to economic and social life.

Methods

Data

We constructed the mobility network using the Seoul "Living Mobility" dataset[19–23] a publicly available, de-identified, and statistically processed resource based on mobile phone data provided by the Seoul Metropolitan Government. This dataset was developed to offer objective insights for improving travel times and enables detailed analysis of movement patterns beyond conventional traffic data. It integrates public big data owned by Seoul, traffic polygon units from the Transport Research Institute, and LTE/5G mobile signal data from KT. It estimates total population movement by extrapolating the mobility of KT users, adjusting for KT's market share and other correction factors, thereby reflecting overall inter-regional mobility rather than that of KT users alone. The dataset captures movement across multiple nodes—public transit, private vehicles, bicycles, and walking—while excluding trips with very short dwell times (e.g., school drop-offs, neighborhood strolls) or minimal travel distances. It only includes movements where either the origin or destination is within Seoul. The data is available from January 2020 including rich attributes such as the time of movement (daily/hourly), origin–destination pairs at the "dong" (administrative division) level, number of travelers, demographic details (age and gender), travel time, and distance.

Mobility network

To construct the mobility network encompassing the entirety of Seoul during the pandemic period (2020–2022), we processed the daily and hourly mobility flow among 424 administrative divisions, known as "dong", based on Seoul's official administrative structure into monthly population level mobility patterns across 25 districts, a larger administrative unit called "gu" (district). On average, a "dong" in Seoul has a population size ranging from approximately $10{,}000$ to $50{,}000$ people and covers an area of $2-5$ square kilometers, while a "gu" typically encompasses $200{,}000$ to $700{,}000$ residents and spans $10-47$ square kilometers, reflecting the diverse and dense urban structure of the city.

We then constructed Seoul Mobility Network (SMN) as a directed, weighted network, denoted as $G=(V,E)$, where nodes (V) represent individual "dong" and edges (E) represent the intensity of mobility among them. The adjacency matrix $W=\{\omega_{i,j}\}_{n\times n}$ defines the graph, where $n=424$ corresponds to the total number of nodes ("dong"). Each element $\omega_{i,j}$ represents the number of people moving from node v_i to node v_j, including cases for self-loops, where $i=j$, reflects within- "dong" mobility. Since our dataset captures comprehensive mobility data across the entirety of Seoul, every "dong" interacts with all others. As a result, the network is fully connected, with all nodes linked by weighted edges representing mobility flows. This construction of the SMN provides a comprehensive and detailed representation of mobility dynamics within Seoul during the pandemic period. The network, comprising 424 nodes and $179{,}776$ $(424{*}424,\ \text{whole connected})$ weighted directed edges, captures both within- and across- "dong" movement patterns, offering an in-depth view of the interconnectedness of Seoul's administrative divisions. Using the SMN, we examined (i) local node intensity via weighted densities within and between districts, (ii) global connectivity intensity through the distribution of node strengths, (iii) community structure by detecting densely interconnected node clusters, and (iv) network hubs, identifying the ten most and least central dongs by standard centrality measures.

Weighted density

Weighted density averages the weights of all existing edges over every possible node pair, describing how heavily connected the entire network is overall. However, since the Seoul Mobility Network (SMN) is fully connected (density = 1), we account for edge weights to capture meaningful variation in connectivity. To apply the notion of density to a weighted graph in this context, we took the sum of weights of the edges divided by a total number of edges, given by the following equation given as: $\lambda_{\,weighted\ \&\ directed}$ $=\frac{\sum_{(i,j)\in E}\omega_{ij}}{E_{max}}$, where E_{max} is the number of all possible edges. Because raw weights ω_{ij} represent population-scale flows, large flows are partly explained by the short distances between adjacent subdistricts. To address this, we computed a distance-adjusted weighted density, replacing each weight by $\omega'_{ij}=\omega_{ij}*d_{ij}$, where d_{ij} is the geographic distance between nodes i and j. This adjustment allows us to highlight these structurally

significant long-range connections while still preserving the population-based meaning of the original edge weights. To gain deeper insights into mobility patterns, we calculated both within-"gu" and across-"gu" densities. Additionally, to explore temporal changes in mobility, we constructed three separate subnetworks, corresponding to years 2020, 2021, and 2022. This comprehensive analysis examines mobility within and across different "gu" (district) while tracking its evolution over time.

Specifically, within- "gu" density quantifies the degree of mobility between "dong" within the same "gu", whereas across- "gu" density captures the extent of mobility between "dong" belonging to different "gu". Unlike the overall network, where the denominator is n^2, the denominators for within- "gu" and across- "gu" densities correspond to the actual numbers of possible edges. For within- "gu" density, the denominator is the number of total edges within the same "gu". For across- "gu" density, the denominator is the number of total edges between "dong" in different "gu". These results are summarized in Table 1, providing a detailed view of the spatial and temporal dynamics of mobility in Seoul for all 25 districts ("gu"). Across the study period, both raw mobility volumes (Figure S1) and their weighted-density mobility patterns rise gradually in every district while maintaining parallel trajectories, indicating stability in the underlying mobility structure despite overall growth in movement. Thus, we summarized annual average weighted densities for each dong in Table 1.

Node strength distribution

For any node, node strength sums the weights of all its incident edges, indicating how intense that node's direct connections are (e.g., total trips into and out of a district). In a directed and weighted network with self-loops, the strength of a node quantifies its total connectivity by summing the weights of all its incoming and outgoing edges, including self-loops. For a given node v_i, its strength is defined as: $s_i = \sum_{i \neq j}(\omega_{ij} + \omega_{ji}) + \omega_{ii}$, where ω_{ij} represents the weight of the edge directed from node v_i to node v_j, ω_{ji} represents the weight of the edge directed from node v_j to node v_i, and ω_{ii} is the weight of the self-loop at node v_i[24,25]. The strength data was calculated by R package "$igraph$"[26]. Understanding the distribution of node strength is crucial for revealing the heterogeneity of mobility pattern and identifying nodes' roles as hubs. Examining whether the distribution follow a power-law can uncover scale-free properties, highlighting the presence of key hubs that dominate movement flows and shape the network's connectivity[27].

To rigorously examine the presence of scale-free properties in the tail of the node strength distribution within the SMN, we applied the method outlined by[28]. This method, accessible via the R package "$poweRlaw$"[29], identifies the threshold (x_{min}) beyond which a power-law distribution applies and estimates the scale parameter (α) of the distribution. By employing a bootstrapping procedure, it also quantifies uncertainties for these parameters and assesses the goodness-of-fit through the Kolmogorov-Smirnov statistic and a bootstrap-derived p-value.

Community detection

Community detection identifies clusters of nodes that are more densely connected to each other than to the rest of the network, revealing underlying modules or functional groups. In the context of urban mobility, it identifies groups of nodes, such as administrative regions or population clusters, that exhibit stronger internal mobility connections compared to those with regions outside the group. We identified communities with the Infomap algorithm using the R package "$igraph$"[26]. Infomap applies the map-equation framework introduced by Rosvall & Bergstrom (2008)[30] and later extended[31], and is well suited to weighted, directed networks with self-loops such as the Seoul Mobility Network. It models information flow as a random walk and partitions the graph so that the expected code length required to describe the walker's path is minimised, following the Minimum Description Length (MDL) principle. Specifically, Infomap minimizes the total code length $L(M)$ required to describe the path of a random walker, defined as: $L(M) = q_{\curvearrowright} H(Q) + \sum_{i=1}^{n} p_{\circlearrowright}^{i} H\left(P^{i}\right)$[30] where M represents a given partition of the network into communities; $q_{\curvearrowright}$ is the total probability of exiting communities; $H(Q)$ is the entropy of inter-community movements; $p_{\circlearrowright}^{i}$ is the total probability of movements within community i; and $H\left(P^{i}\right)$ is the entropy of intra-community movements. By minimizing $L(M)$, Infomap simultaneously determines both the optimal number of communities and their membership, without any need to pre-specify these parameters.

The communities were ranked based on the number of "dongs" they included. In order to better understand the spatial distribution of mobility communities and their geographic patterns, we created a map to visualize the spatial distribution of communities detected in the SMN, with each community assigned a distinct color. The map is based on the administrative boundaries of Seoul and uses data from the GitHub repository called "southkorea-maps" (South Korea Maps, 2018)[32]. This visualization helps to identify spatial clusters of mobility patterns and provides an intuitive way to understand the geographic distribution of community-level interactions. The map was generated using the R package "$ggplot2$"[33], with administrative boundaries processed through the R package "$geojsonio$"[34]. Community memberships were integrated into the map by merging detection results with spatial data, and the boundaries of districts ("gu") were highlighted to indicate broader administrative regions. To further examine the interactions between and within communities, we calculated the weighted density for all community pairs. This analysis offers valuable insights into how mobility is distributed across different communities.

Centrality

Centrality quantifies how important or influential each node is—based on criteria such as how many connections it has, how often it sits on shortest paths, or how quickly it can reach others—thereby pinpointing key hubs or mediators in the network. We analyzed the centrality of Seoul's "dong" within SMN using th Weihted PageRank

Districts (Gu)	Population in 2020 (in thousands)	Number of dongs	Within-"gu" weighted density				Across-"gu" weighted density			
			2020	2021	2022	% Change (2020–2022)	2020	2021	2022	% Change (2020–2022)
Songpa	667	27	418516 (0.96)	456406 (0.96)	505269 (0.95)	+20.7%	97095 (1.01)	101405 (1.01)	111514 (1.02)	+14.9%
Gangseo	580	20	639713 (1.46)	709853 (1.49)	797494 (1.50)	+24.7%	93492 (0.97)	98404 (0.98)	105791 (0.97)	+13.2%
Gangnam	539	22	712690 (1.63)	766968 (1.61)	864061 (1.62)	+21.2%	188305 (1.95)	196330 (1.95)	210610 (1.93)	+11.8%
Nowon	517	19	558313 (1.28)	603177 (1.27)	668074 (1.26)	+19.7%	92847 (0.96)	94990 (0.94)	100654 (0.92)	+8.4%
Gwanak	503	21	314152 (0.72)	330471 (0.70)	372269 (0.70)	+18.5%	75477 (0.78)	77986 (0.78)	84864 (0.78)	+12.4%
Eunpyeong	477	16	609529 (1.39)	654972 (1.38)	739759 (1.39)	+21.4%	80930 (0.84)	83047 (0.83)	88803 (0.82)	+9.7%
Gangdong	455	18	623248 (1.43)	682328 (1.44)	733309 (1.38)	+17.7%	84748 (0.88)	90057 (0.90)	95931 (0.88)	+13.2%
Yangcheon	451	18	315564 (0.72)	343361 (0.72)	368031 (0.69)	+16.6%	65539 (0.68)	67228 (0.67)	70400 (0.65)	+7.4%
Seongbuk	443	20	278133 (0.64)	306072 (0.64)	341595 (0.64)	+22.8%	68946 (0.72)	71941 (0.72)	77656 (0.71)	+12.6%
Seocho	418	18	605795 (1.39)	657358 (1.38)	723223 (1.36)	+19.4%	156834 (1.63)	160890 (1.60)	171110 (1.57)	+9.1%
Guro	408	15	390550 (0.89)	427678 (0.90)	474190 (0.89)	+21.4%	90104 (0.93)	94161 (0.94)	100954 (0.93)	+12.0%
Yeongdeungpo	402	18	370556 (0.85)	417345 (0.88)	468823 (0.88)	+26.5%	115911 (1.20)	124321 (1.24)	136988 (1.26)	+18.2%
Dongjak	395	15	304933 (0.70)	345251 (0.73)	394087 (0.74)	+29.2%	84894 (0.88)	87851 (0.87)	96117 (0.88)	+13.2%
Jungnang	394	16	409831 (0.94)	448140 (0.94)	503986 (0.95)	+23.0%	70919 (0.74)	74274 (0.74)	78781 (0.72)	+11.1%
Mapo	379	16	525798 (1.20)	561377 (1.18)	637722 (1.20)	+21.3%	114797 (1.19)	119213 (1.19)	132470 (1.22)	+15.4%
Gwangjin	355	15	446090 (1.02)	477423 (1.00)	564323 (1.06)	+26.5%	86757 (0.90)	90915 (0.90)	100474 (0.92)	+15.8%
Dongdaemun	354	14	421629 (0.96)	457867 (0.96)	521534 (0.98)	+23.7%	90167 (0.94)	95105 (0.95)	104095 (0.96)	+15.4%
Dobong	320	14	403168 (0.92)	430747 (0.91)	467086 (0.88)	+15.9%	72246 (0.75)	74878 (0.74)	78653 (0.72)	+8.9%
Seodaemun	319	14	356905 (0.82)	392104 (0.83)	432033 (0.81)	+21.0%	92716 (0.96)	94303 (0.94)	103818 (0.95)	+12.0%
Gangbuk	304	13	546674 (1.25)	577555 (1.22)	633836 (1.19)	+15.9%	77555 (0.80)	80225 (0.80)	84461 (0.78)	+8.9%
Seongdong	294	17	241939 (0.55)	269562 (0.57)	311593 (0.59)	+28.8%	75642 (0.78)	81542 (0.81)	87818 (0.81)	+16.1%
Geumcheon	245	10	550912 (1.26)	579332 (1.22)	611679 (1.15)	+11.0%	78166 (0.81)	82472 (0.82)	85737 (0.79)	+9.7%
Yongsan	238	16	277312 (0.63)	302971 (0.64)	345113 (0.65)	+24.4%	75954 (0.79)	81581 (0.81)	90566 (0.83)	+19.2%
Jongno	155	17	212315 (0.49)	232108 (0.49)	295147 (0.55)	+39.0%	110772 (1.15)	115088 (1.14)	131414 (1.21)	+18.6%
Jung	132	15	236176 (0.54)	254704 (0.54)	299788 (0.56)	+26.9%	132094 (1.37)	136518 (1.36)	151333 (1.39)	+14.6%
Total	9746	424	437266 (1.00)	475252 (1.00)	532084 (1.00)	+21.7%	96389 (1.00)	100529 (1.00)	108945 (1.00)	+13.0%

Table 1. Within/ across weighted mobility densities in Seoul (2020–2022).
Values in parentheses show each district's density relative to the citywide mean. For Songpa in 2020: (1) **Within-gu density**: Total flow among Songpa's 27 dongs (293,798,232) ÷ possible directed dong–dong pairs without self-loop ($27 \times 26 = 702$) = 418,516. Compared with the citywide intra-gu average (437,266) gives the reported ratio 0.96; (2) **Across-gu density**: Total flow between Songpa and all other districts (2,083,852,890) ÷ possible directed inter-district edges ($2 \times 27 \times [424 - 27] = 21{,}462$) = 97,095. Compared with the citywide across-gu average (96,389), this yields 1.01. The color scale represents each district's weighted density relative to the Seoul-wide mean (normalized to 1). Cells in blue indicate values below the city mean (negative deviation), light gray marks values approximately equal to the city mean (= 1), and orange denotes values above the city mean (positive deviation).

(WPR) measure, implemented via the R package "$wdnet$"[35]. WPR is an extension of the traditional PageRank algorithm that incorporates edge weights "ω" to reflect the strength of connections between nodes. Specifically, WPR assigns a score to each node based on the weighted sum of connections, where both the quantity of connections and the importance of connected nodes influence the score. In the context of SMN, this method highlights key "dongs" that play a central role in movement dynamics, capturing both their direct mobility flows and their connectivity to other influential nodes. By applying WPR, we identified the ten most and ten least influential "dongs" in the SMN, as shown in Table 2.

Model visualization

All the maps were generated using R software (version 4.5.0)[36] with the packages $ggplot2$ [33] and "sf"[37] for spatial visualization. Seoul administrative boundary shapefiles were obtained from the open-source GitHub repository "southkorea-maps" (South Korea Maps, 2018)[32]. All visualizations were generated by the authors. The monthly network patterns remain stable throughout 2020–2022, confirmed by the modularity, assortativity, and pairwise Adjusted Rand Index (ARI)[38] metrics. Thus, we reported three-year aggregated node strengths, community clustering, and centrality results in the following section. Yearly aggregated network metrics are shown in Figure S2 and Table S1.

Result

The overall mobility trends across 424 subdistricts ("dong") in Seoul's 25 districts ("gu"), treating each district independently to allow comparability, indicate a steady rise in weighted flows—defined as the number of movers multiplied by their travel distance—between 2020 and 2022 (Figure S1). At the citywide level, within-gu weighted density increased by + 21.7%, while across-gu weighted density rose by + 13.0%, underscoring the faster recovery of localized mobility once restrictions eased. However, district-level patterns diverged, mirroring each area's role as either a commercial-institutional hub or a more residential, peripheral zone. Gangnam, Seocho, and Mapo sustained both within- and across-district densities well above the city average (ratios > 1), indicating their central roles in both local and inter-district mobility. These districts are known for being major commercial and business hubs in Seoul, which explains their elevated mobility levels both internally and externally. In contrast, districts such as Jongno and Jung maintain consistently low within-gu densities (ratios < 0.6) yet have high across-gu densities (ratios > 1.1), suggesting that while local movement within these districts is limited, they serve as key transit or urban cores for people from other districts—likely due to their administrative and historical significance. On the other hand, Eunpyeong and Gangdong display a pattern of high within-gu densities (ratios around 1.4) but relatively low across-gu densities (ratios < 0.9), implying strong localized movement but less integration with the broader city network—possibly reflecting self-contained residential zones on the urban periphery. Finally, Gwanak, Seongbuk, and Yangcheon consistently showed low within- and across-gu densities

Rank	Top 10 subdistricts ("dongs")				
	Subdistrict ("dong")	**District ("gu")**	**Community**	**Strength**	**Mobility (%)**
1	Yeoksam	Gangnam	4	432.98	3.05%
2	Yeoui	Yeongdeungpo	1	351.65	2.47%
3	Jongno1_2_3_4Ga	Jongno	3	343.88	2.42%
4	Seogyo	Mapo	3	295.97	2.08%
5	Seocho	Seocho	4	254.72	1.79%
6	Sinchon	Seodaemun	3	213.80	1.50%
7	Myeong	Jung	3	203.41	1.43%
8	Yeongdeungpo	Yeongdeungpo	1	191.91	1.35%
9	Hangangno	Yongsan	10	172.53	1.21%
10	Samseong	Gangnam	4	181.41	1.28%
Rank	Bottom 10 subdistricts ("dongs")				
	Subdistrict ("dong")	District ("gu")	Community	Strength	Mobility (%)
424	Dunchon	Gangdong	9	5.68	0.04%
423	Changsin	Jongno	5	8.30	0.06%
422	Ichon	Yongsan	10	11.20	0.08%
421	Singil	Yeongdeungpo	1	11.78	0.08%
420	Sinwol	Yangcheon	6	11.88	0.08%
419	Cheongnim	Gwanak	1	14.96	0.11%
418	Garibong	Guro	1	14.93	0.10%
417	Banpobon	Seocho	4	17.26	0.12%
416	Muwak	Jongno	3	17.14	0.12%
415	Hongje	Seodaemun	3	18.18	0.13%

Table 2. Top and bottom 10 subdistricts ("dongs") ranked by weighted page rank. Strength is reported in million. Mobility (%) represents the proportion of total mobility associated with the corresponding dong.

(ratios < 0.8) throughout the study period, underscoring their spatial marginality in Seoul's mobility network; both districts are largely residential and lack major commercial or institutional hubs.

Figure 1a illustrates the empirical survival function for node strength, presented on a log-log scale. In this context, the term "survival" refers to the complement of the cumulative distribution function (1 - CDF). It represents the proportion of nodes with strength values greater than a given threshold. A scale-free property is indicated when the tail of the plot exhibits a nearly linear relationship. The results show that scale-free behavior emerges at high mobility values (greater than 73 million), whereas nodes with lower mobility volumes follow a different distribution pattern. These high-mobility nodes (key "dongs") play an outsized role in the network's connectivity, suggesting their critical importance in mobility dynamics.

The Kolmogorov-Smirnov test yielded a p-value of 0.46, indicating no evidence to reject the power-law model above this threshold. The estimated threshold was $x_{min} = 73$ (standard error: 8.81), as shown in Fig. 1 (a), and the scale parameter was $\alpha = 3.71$ (standard error: 0.30). Notably, 138 out of 424 nodes (33%) have strength values exceeding this threshold, accounting for 56% of the total strength, representing the highly active "dongs" that dominate mobility flows. These findings demonstrate that node strength distribution in the SMN display scale-free behavior in its tail. This pattern highlights the dominance of highly active "dongs" in driving mobility flows, while the majority of nodes with lower mobility volumes follow a more varied and non-power-law distribution. The presence of a power-law tail underscores the critical role of these hubs in shaping the network's overall structure and dynamics. The results were shown in Fig. 1(b), illustrating hub 'dongs' (highlighted in pink) across districts, revealing highly heterogeneous coverage patterns of these hub areas within each district.

Figure 2a shows that applying the Infomap community-detection algorithm to 2020–2022 mobility data identified 11 communities (C-1–C-11) during the COVID-19 pandemic. The result reveals distinct "community clusters" within Seoul, indicating that certain districts share stronger connections or similarities with each other than they do with other parts of the city. Each cluster consists of one to five districts (gu) but does not strictly align with administrative boundaries. Such clustering can arise from various factors—like geographic proximity, population movement patterns (e.g., commuting flows, public transit hubs), or socio-demographic similarities (income levels)—and suggests that these clusters function somewhat independently in terms of internal flows or interactions—people often work, shop, or attend school within nearby areas. Figure S2 presents the community-detection maps for each year.

Such clustering mobility patterns are illustrated through the within and across density matrix, as shown in Fig. 2b, among the eleven communities. First, the within cluster density of each community was 50 to 400 times greater than across cluster density. For example, Community 9 (Gangdong-gu & Part of Songpa-gu) shows the highest Within-Cluster mobility density driven by a robust residential community, good transportation infrastructure, abundant local amenities, and an environment conducive to meeting most daily needs locally. On the other hand, Community 1 (Guro, Geumcheon, Yeongdeungpo, Dongjak, Gwanak) or Communities 2 & 5 show lower Within-Cluster mobility density than other communities. Community 9 (and 8 and 11)'s high internal mobility density is largely explained by well-connected transit routes, a strong family-focused environment, and a growing local economy—factors that encourage residents to stay within these districts for both work and leisure. Both Gangdong-gu and Songpa-gu are known for large-scale apartment complexes and well-planned neighborhoods with ample retail, dining, and recreational options. This layout encourages residents to stay within the area for everyday needs. On the other hand, relative to Seoul's upscale southeastern districts, areas in the southwest (Community 1) often have a more mixed-income population, affordable housing, and a balance of factory (Guro and Geumcheon)/office employment and residential neighborhoods and commercial hubs (Yeongdeungpo, Dongjak, and Gwanak), contributing to frequent short-distance travel between them. In terms of Across-Cluster mobility density, Community 4 shows high across-community mobility density, driven primarily by its central role in Seoul's economic and cultural life. With dense commercial, residential,

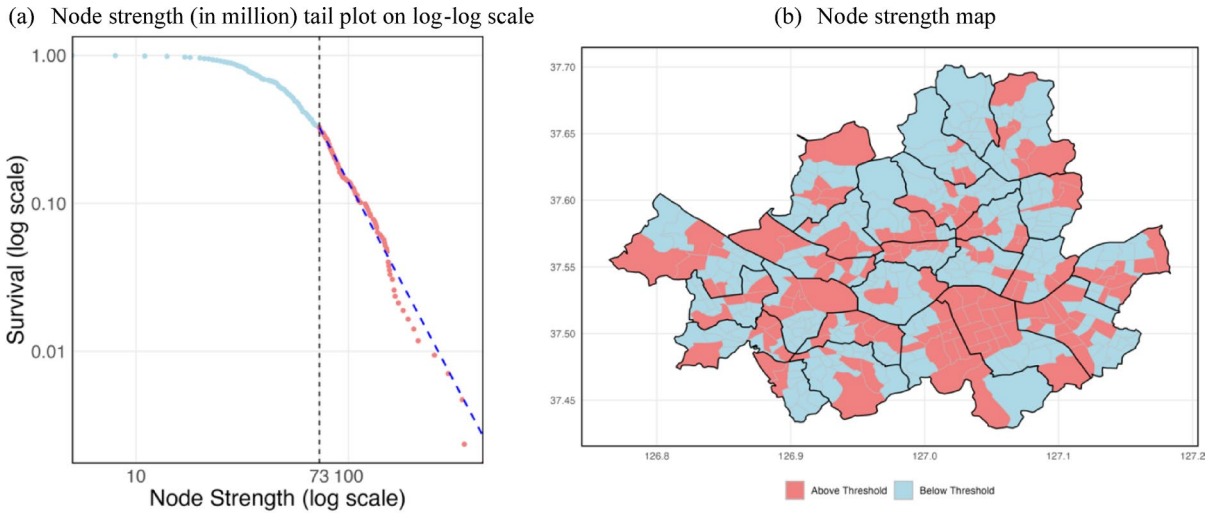


Fig. 1. Node strength (in million) tail plot and map.

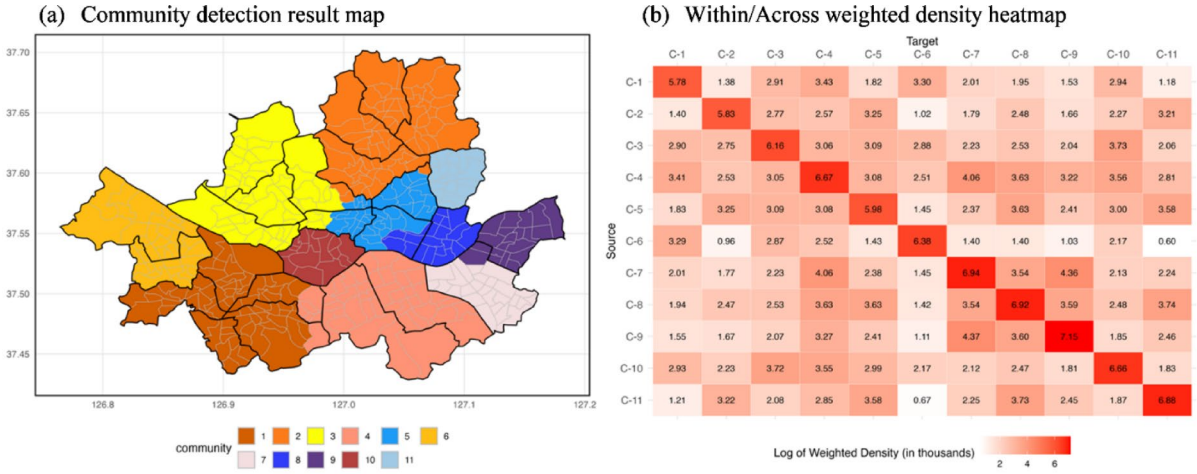


Fig. 2. Community detection map and within/across weighted density matrix heatmap.

and educational facilities, it attracts diverse travelers from virtually every corner of the city. On the other hand, Community 6's lower cross-boundary density reflects its more peripheral location, self-sufficient residential character, and comparatively fewer large-scale business or entertainment hubs. Table S2 shows demographic, economic, and mobility profiles of the 11 detected mobility communities in Seoul.

As shown in Table 2, the top 10 and bottom 10 subdistricts ("dong") ranked by Weighted PageRank (WPR) reveal 10 to 70 times higher mobility strengths in top ranked dongs than the bottom-ranked, highlighting the dominance of business districts over primarily residential areas. For example, Yeoksam-dong (Gangnam-gu), Yeoui-dong (Yeongdeungpo-gu), and Jongno1_2_3_4Ga (Jongno-gu) show high movement and connectivity, while dongs such as Dunchon-dong (Gangdong-gu), Changsin-dong (Jongno-gu), and Ichon-dong (Yongsan-gu) register much lower mobility, reflecting disparities in economic activity and urban function. For example, Yeoksam-dong, ranked first, as the highest strength of 432.98 million movements (3.05% of total mobility) reflects its role as a home to major corporate headquarters, financial institutions, and tech startups along Teheran-ro. Yeoui-dong, the second-ranked, serves as Seoul's financial and political hub, hosting the National Assembly, major banks, and broadcasting companies, with 351.65 million movements (2.47% of mobility. Jongno1_2_3_4Ga, in central Seoul, ranks third with 343.88 million movements (2.42%), acting as a critical transit and economic node by integrating government offices, corporate headquarters, and retail zones. Conversely, the lowest-ranked dongs exhibit minimal movement. Dunchon-dong (Gangdong-gu) records only 5.68 million movements (0.04% of total), reflecting its primarily residential nature with few commercial or transport hubs. Changsin-dong (Jongno-gu) has 8.30 million movements (0.06%), characterized by its older, low-density structures and traditional workshops. Ichon-dong (Yongsan-gu), with 11.20 million movements (0.08%), is a relatively isolated neighborhood near the Han River, mainly composed of high-end residences, limiting its broader citywide role. These suggest that public health interventions should prioritize high-mobility hubs and their belonged community clusters, which are likely to serve as critical nodes for disease transmission and economic activity, while tailored strategies may be needed in low-mobility areas to address potential disparities in service access. Figure S3 displays the geographic distribution of the 10 highest- and 10 lowest-ranked subdistricts.

Discussion

This study assessed the comprehensive mobility network structure in Seoul during the COVID-19 pandemic from 2020 to 2022 by applying complex network analysis. Seoul's mobility network remained fully connected yet highly heterogeneous, with central hubs and clusters dominating movement. Within-dong mobility increased more rapidly than across-dong mobility (21.7% vs. 13.0%) over the study period. Node strength distribution showed 138 high-mobility dongs (33%) driving 56% of total flows. Community detection identified 11 clusters transcending district boundaries, with within-community mobility 2–5 times higher than cross-community flows. High-mobility hubs, such as Yeoksam-dong (Gangnam-gu) and Yeoui-dong (Yeongdeungpo-gu), exhibited up to 70 times more movement than peripheral areas. By focusing on high-mobility hubs (e.g., Yeoksam-dong), leveraging cluster-based strategies, and addressing low-mobility peripheral areas, policymakers can design targeted, efficient, and equitable interventions.

The weighted density (Table 1), which normalizes for network structure and distance, shows that within-dong flows (e.g., local streets and bus routes) are far more saturated than cross-dong flows, despite the latter's larger volume (Figure S1). Weighted density highlights areas of high interaction intensity, which is critical for public health (e.g., identifying local transmission hotspots) and urban planning (e.g., targeting congestion relief in heavily utilized local networks), in ways that raw flows alone cannot capture. The rising saturation of within-dong flows during the COVID-19 pandemic years reflects intensified local interactions, underscoring the growing importance of clustering and localized hotspots in shaping transmission risks under the Omicron era (Figure S4). This finding demonstrates that effective monitoring of social distancing policies requires moving beyond simple mobility reduction metrics to examine network structure changes such as community clustering

and local hubs. Despite declines in overall mobility, the persistence of stable connectivity reveals the resilience of Seoul's urban mobility system, implying that blanket restrictions may be less effective than anticipated. Instead, differentiated approaches are needed[39]: districts with strong within-dong saturation should prioritize intra-community risks in settings like apartment complexes and markets, while those with high across-dong flows should focus on inter-district transmission. Moreover, public health authorities could focus interventions on the 138 high-mobility "dongs" that account for more than half of all movement. Such targeted strategies—strengthening testing, vaccination, or communication in high-risk hubs, and ensuring equitable access in low-mobility dongs—can more effectively balance epidemic control with minimizing social and economic disruption[8,40,41]. By recognizing both resilience and heterogeneity, this structural perspective provides a critical foundation for sustainable and equitable public health policies[42].

Our results both complement and extend previous COVID-19 mobility research. In cities under strict lockdowns, other studies have shown major structural reconfigurations in movement networks[11,43]. For example, "who goes where" patterns were dramatically altered—likely involving the disappearance of certain travel routes, the emergence of new ones, and significant shifts in the relative importance of various destinations[15]. Other studies in Paris, Shenzhen and 25 major U.S. cities showed COVID-19 shattered the dominance of traditional downtown hubs, whose mobility networks fragmented into smaller, geographically tight communities while long-distance links weakened under lockdown and only partly restored their pre-pandemic hierarchies[15,44,45]. By contrast, even at a monthly resolution, Seoul's network remained structurally stable (Figure S2), with only the overall intensity of movement fluctuating over time. These outcomes reflect South Korea's pandemic management, which relied on targeted interventions - likely including extensive testing, contact tracing, and isolation of specific cases or clusters, while allowing most daily activities to continue with precautions. Consistent with Kim and Jun (2022), the fundamental inflow and outflow patterns of Seoul appear robust despite pandemic conditions[18]; however, our dong-level analysis adds granularity by highlighting specific areas/hubs and identifying how community clusters are maintained and connected during the pandemic, offering valuable insights beyond the broader city-level analysis of previous research[8,46]. To our knowledge, this is the first study informing public health policy based on within and across connectivity and clustering patterns and hubs/marginal areas. While many studies during the pandemic examined mobility patterns based on telecommunications data, it is rare for public datasets to provide mobility data that can be constructed to create origin–destination (OD) matrices at the county or township level across an entire state. We suggest that other cities and regions also generate and release such public data on a regular basis. These datasets would not only offer an important baseline for preparing against future pandemics but also serve as valuable resources for policy monitoring and urban planning purposes.

Our study has some limitations. First, as our analysis focuses exclusively on Seoul, the findings may not readily generalize to other urban contexts with differing transportation infrastructures or socioeconomic profiles. Applying our approach in diverse contexts—such as rural areas, nationwide patterns, or long-term trends—may yield additional insights into the underlying pattern or causes of social disparity. Second, our study could not directly assess the relationship between mobility and COVID-19 incidence due to inconsistent data resolutions: incidence data were available at the 25-gu (district) level, whereas mobility data were collected at the finer 424-dong (subdistrict) level. Incidence peaks also occurred almost simultaneously across all gus in this tightly connected metropolis, leaving insufficient temporal variation to test how directed and weighted flows shape transmission. However, annual incidence trends (Figure S4) indicate that transmission was higher in city centers during the early pandemic (2020) but gradually shifted to outer districts by 2022. This shift mirrors the rise in localized mobility density, suggesting that early spread was driven by long-distance, inter-district travel focused on commercial hubs, whereas later transmission was sustained largely by short-distance, intra-district movements. Third, our study cannot explain the drivers of the observed heterogeneity or regional disparities in mobility patterns. We did not include node- or edge-level attributes like inter-dong distance or resident/worker population in our network analysis; incorporating distance could down-weight short trips and emphasize long-range "bridge" corridors, potentially narrowing within-district density advantages and highlighting strategic cross-district links, while normalizing by population might shift node strength to a per-capita basis, reducing the prominence of large residential districts and elevating smaller, highly active commercial hubs. Fourth, community detection results can be influenced by the choice of algorithm. We used Infomap because it is particularly well-suited for directed, weighted networks with self-loops, which closely reflect the characteristics of our mobility data. Although partitions might slightly differ under alternative algorithms, identifying highly connected clusters and hubs remains a useful way to characterize Seoul's mobility network, and thus our findings still provide valuable insights for public health and urban planning. Future research may incorporate socioeconomic factors (node attributes) or demographic characteristics (edge attributes) into the network analyses, which help understand the underlying causes of mobility dynamics or geographical heterogeneity[47,48]. By marrying who moves where (network analytics) with who is vulnerable (socio-economic maps), city planners can anticipate—and not merely react to—the shifting geography of COVID-19 and future respiratory epidemics. Nevertheless, our findings remain robust in capturing the structural stability and heterogeneity of Seoul's mobility network, adding value by identifying key hubs and community clusters to inform targeted public health and urban planning strategies.

Conclusion

This study assessed the comprehensive mobility network structure in Seoul during the COVID-19 pandemic from 2020 to 2022 by applying complex network analysis. By investigating mobility flows among Seoul's 424 dongs during COVID-19, our findings show Seoul's mobility network remained fully connected yet highly heterogeneous, with central hubs and clusters dominating movement. Identifying these hubs and clusters provides crucial insights for targeted disease control strategies in densely populated urban areas, while

minimizing social disruption. Conversely, identifying low-mobility dongs helps reveal potential disparities in service access, highlighting areas where tailored interventions are necessary.

Data availability

All the processed data and code can be found at (https://github.com/UConn-Health-Disease-Modeling/SeoulMobilityNetwork).

Received: 31 May 2025; Accepted: 20 December 2025
Published online: 30 January 2026

References

1. Zhang, M. et al. Human mobility and COVID-19 transmission: a systematic review and future directions. *Ann. Gis.*. **28**, 501–514 (2022).
2. Barbosa, H. et al. Human mobility: models and applications. *Phys. Rep.* **734**, 1–74 (2018).
3. Jiang, S. et al. The TimeGeo modeling framework for urban mobility without travel surveys. *Proc. Natl. Acad. Sci.* **113**, E5370–E5378 (2016).
4. Kraemer, M. U. G. et al. The effect of human mobility and control measures on the COVID-19 epidemic in China. *Science* **368**, 493–497 (2020).
5. Zhao, S. et al. The association between domestic train transportation and novel coronavirus (2019-nCoV) outbreak in China from 2019 to 2020: a data-driven correlational report. *Travel Med. Infect. Dis.* **33**, 101568 (2020).
6. González, M. C., Hidalgo, C. A. & Barabási, A-L. Understanding individual human mobility patterns. *Nature* **453**, 779–782 (2008).
7. Wesolowski, A. et al. Quantifying the impact of human mobility on malaria. *Science* **338**, 267–270 (2012).
8. Chang, S. et al. Mobility network models of COVID-19 explain inequities and inform reopening. *Nature* **589**, 82–87 (2021).
9. de Jong, B. C. et al. Ethical considerations for movement mapping to identify disease transmission Hotspots - 25, Emerging infectious diseases journal - CDC. https://doi.org/10.3201/eid2507.181421 (2019).
10. Lee, E. C., Arab, A., Colizza, V. & Bansal, S. Spatial aggregation choice in the era of digital and administrative surveillance data. *PLOS Digit. Health*. **1**, e0000039 (2022).
11. Schlosser, F. et al. COVID-19 lockdown induces disease-mitigating structural changes in mobility networks. *Proc. Natl. Acad. Sci.* **117**, 32883–32890 (2020).
12. Badr, H. S. et al. Association between mobility patterns and COVID-19 transmission in the USA: a mathematical modelling study. *Lancet Infect. Dis.* **20**, 1247–1254 (2020).
13. Jia, J. S. et al. Population flow drives spatio-temporal distribution of COVID-19 in China. *Nature* **582**, 389–394 (2020).
14. Lucchini, L. et al. Living in a pandemic: adaptation of individual mobility and social activity in the US., published online Aug 17. https://doi.org/10.48550/arXiv.2107.12235 (2021).
15. Li, S., Chen, P., Hui, F. & Gong, M. Evaluating urban vitality and resilience under the influence of the COVID-19 pandemic from a mobility perspective: A case study in Shenzhen, China. *J. Transp. Geogr.* **117**, 103886 (2024).
16. Marlow, T., Makovi, K. & Abrahao, B. Neighborhood isolation during the COVID-19 pandemic. *Sociol. Sci.* **8**, 170–190 (2021).
17. Park, Y. J. et al. Contact tracing during coronavirus disease outbreak, South korea, 2020 - 26, Emerging infectious diseases journal - CDC. https://doi.org/10.3201/eid2610.201315 (2020).
18. Kim, Y-L. & Jun, B. Inside out: human mobility big data show how COVID-19 changed the urban network structure in the Seoul metropolitan area. *Camb. J. Reg. Econ. Soc.* **15**, 537–550 (2022).
19. Seoul. 'Living Mobility' dataset., https://data.seoul.go.kr/dataVisual/seoul/seoulLivingMigration.do (2025).
20. Kim, H. The sociopolitical context of the COVID-19 response in South Korea. *BMJ Glob Health*. **5**, e002714 (2020).
21. Lim, B., Kyoungseo Hong, E., Mou, J. & Cheong, I. COVID-19 in korea: success based on past failure*. *Asian Econ. Pap.* **20**, 41–62 (2021).
22. Yoo, K. J., Kwon, S., Choi, Y. & Bishai, D. M. Systematic assessment of South korea's capabilities to control COVID-19. *Health Policy Amst Neth.* **125**, 568–576 (2021).
23. Hong, S. A. Toward better pandemic governance and preparedness: South korea's whole-of-nation approach to COVID-19. *BMC Public. Health*. **24**, 2126 (2024).
24. Barrat, A., Barthélemy, M., Pastor-Satorras, R. & Vespignani, A. The architecture of complex weighted networks. *Proc. Natl. Acad. Sci.* **101**, 3747–3752 (2004).
25. Newman, M. E. J. Analysis of weighted networks. *Phys. Rev. E.* **70**, 056131 (2004).
26. Csárdi, G. & Nepusz, T. The igraph software package for complex network research. https://www.semanticscholar.org/paper/The-igraph-software-package-for-complex-network-Cs%C3%A1rdi-Nepusz/1d2744b83519657f5f2610698a8ddd177ced4f5c (Accessed on 9 Dec 2024). (2006).
27. Barabási, A-L. & Albert, R. Emergence of scaling in random networks. *Science* **286**, 509–512 (1999).
28. Clauset, A., Shalizi, C. R. & Newman, M. E. J. Power-Law distributions in empirical data. *SIAM Rev.* **51**, 661–703 (2009).
29. Gillespie, C. S. Fitting heavy tailed distributions: the powerlaw package. *J. Stat. Softw.* **64** https://doi.org/10.18637/jss.v064.i02 (2015).
30. Rosvall, M. & Bergstrom, C. T. Maps of random walks on complex networks reveal community structure. *Proc. Natl. Acad. Sci.* **105**, 1118–1123 (2008).
31. Rosvall, M., Axelsson, D. & Bergstrom, C. T. The map equation. *Eur. Phys. J. Spec. Top.* **178**, 13–23 (2009).
32. Park, L. & Jang, S-H. Southkorea-maps: South Korea administrative divisions in ESRI Shapefile, GeoJSON and TopoJSON formats. https://github.com/southkorea/southkorea-maps (Accessed on 9 Dec 2024). (2018).
33. Villanueva, R. A. M. & Chen, Z. J. ggplot2: elegant graphics for data analysis. *Meas. Interdiscip Res. Perspect.* **17**, 160–167 (2019).
34. Chamberlain, S., Teucher, A. & Mahoney, M. Geojsonio: convert data from and to 'GeoJSON' or 'TopoJSON'., 0 .11.3. (2015).
35. Yuan, Y., Wang, T., Yan, J. & Zhang, P. Generating general Preferential attachment networks with R package Wdnet. *J. Data Sci.* 538–556. (2023).
36. R Core Team. R: The R Project for Statistical Computing., https://www.r-project.org/ (2025).
37. Pebesma, E. Simple features for R: standardized support for Spatial vector data. *R J.* **10**, 439 (2018).
38. Rand, W. M. Objective criteria for the evaluation of clustering methods. *J. Am. Stat. Assoc.* **66**, 846–850 (1971).
39. Hu, Z., Chang, W., Jang, Y., Jo, Y. & Jung, J. Dynamic interactions of COVID-19 incidences, mobility, and social distancing policies in seoul: A VAR model approach. *Sci. Rep.* **15**, 24288 (2025).
40. Yang, S., Senapati, P., Wang, D., Bauch, C. T. & Fountoulakis, K. Targeted pandemic containment through identifying local contact network bottlenecks. *PLOS Comput. Biol.* **17**, e1009351 (2021).
41. Buchel, O., Ninkov, A., Cathel, D., Bar-Yam, Y. & Hedayatifar, L. Strategizing COVID-19 lockdowns using mobility patterns. *R Soc. Open. Sci.* **8**, 210865 (2021).
42. Zhang, X-X. et al. Infectious disease control: from health security strengthening to health systems improvement at global level. *Glob Health Res. Policy*. **8**, 38 (2023).

43. Klein, B. et al. Characterizing collective physical distancing in the U.S. During the first nine months of the COVID-19 pandemic. *PLOS Digit. Health*. **3**, e0000430 (2024).
44. Fanticelli, H. C. et al. Data-driven mobility analysis and modeling: typical and confined life of a metropolitan population. *ACM Trans. Spat. Algorithms Syst.* **8**, 23:1–2333 (2022).
45. Marlow, T., Makovi, K. & Abrahao, B. Durable change in U.S. Urban mobility Networks, 2019–2022. *Socius* **9**, 7 (2023).
46. Zhou, J., Zhao, Z., Zhou, J. & Quantifying COVID-19 transmission risks based on human mobility data: a personalized PageRank approach for efficient contact-tracing. ; published online Oct 3. https://doi.org/10.48550/arXiv.2210.01005 (2022).
47. Casaburi, P. et al. Resilience of mobility network to dynamic population response across COVID-19 interventions: evidences from Chile. *PLOS Comput. Biol.* **21**, e1012802 (2025).
48. Gao, S., Rao, J., Kang, Y., Liang, Y. & Kruse, J. Mapping county-level mobility pattern changes in the united States in response to COVID-19. *SIGSPATIAL Spec.* **12**, 16–26 (2020).

Author contributions

conceptualization: Y.J., Z.H.data curation: Z.H., Y.J., S.S., Y.O.Jformal analysis: Z.H.funding acquisition: J.J.investigation: J.J., Y.J.methodology: Z.H., Y.J.project administration: Z.H., M.Y.resources, software: Z.H.supervision: Y.J., J.J.validation: Y.J.visualization: Z.H.writing – original draft: Z.H., M.Y., Y.J.writing – review & editing: Y.J., S.S., Y.O.J, J.J.

Funding

Grant of the project for Infectious Disease Medical Safety, funded by the Ministry of Health & Welfare, Republic of Korea (grant number: HG22C0094) and Korea Health Technology R&D project through the Korea Health Industry Development Institute (KHIDI), funded by the National Institute of Infectious Diseases, National Institute of Health Republic of Korea (grant number: HD22C2045).

Declarations

Competing interests

The authors declare no competing interests.

Additional information

Supplementary Information The online version contains supplementary material available at https://doi.org/10.1038/s41598-025-33655-7.

Correspondence and requests for materials should be addressed to J.J. or Y.J.

Reprints and permissions information is available at www.nature.com/reprints.

Publisher's note Springer Nature remains neutral with regard to jurisdictional claims in published maps and institutional affiliations.

Open Access This article is licensed under a Creative Commons Attribution-NonCommercial-NoDerivatives 4.0 International License, which permits any non-commercial use, sharing, distribution and reproduction in any medium or format, as long as you give appropriate credit to the original author(s) and the source, provide a link to the Creative Commons licence, and indicate if you modified the licensed material. You do not have permission under this licence to share adapted material derived from this article or parts of it. The images or other third party material in this article are included in the article's Creative Commons licence, unless indicated otherwise in a credit line to the material. If material is not included in the article's Creative Commons licence and your intended use is not permitted by statutory regulation or exceeds the permitted use, you will need to obtain permission directly from the copyright holder. To view a copy of this licence, visit http://creativecommons.org/licenses/by-nc-nd/4.0/.

© The Author(s) 2026